World Academy of Science, Engineering and Technology
International Journal of Mechanical and Mechatronics Engineering
Vol:8, No:12, 2014

Stress Concentration around Countersunk Hole in Isotropic Plate under Transverse Loading

Parveen K. Saini, Tarun Agarwal

***Abstract*—**An investigation into the effect of countersunk depth, plate thickness, countersunk angle and plate width on the stress concentration around countersunk hole is carried out with the help of finite element analysis. The variation of stress concentration with respect to these parameters is studied for three types of loading viz. uniformly distributed load, uniformly varying load and functionally distributed load. The results of the finite element analysis are interpreted and some conclusions are drawn. The distribution of stress concentration around countersunk hole in isotropic plates simply supported at all the edges is found similar and is independent of loading. The maximum stress concentration also occurs at a particular point irrespective of the loading conditions.

***Keywords*—**Stress Concentration Factor, Countersunk hole, Finite element, ANSYS**.**

I. Introduction

THE advancement of technology has led to a trend towards greater speed and complexity of machinery, greater size and diversity of structures, and greater economy and refinement of design. Keeping in mind the durability of the machinery, safety of structures etc., one must be aware of the stresses that develop in them. Thus, the need for more accurate methods of stress analysis becomes inevitable. This study has been carried out to predict the stress concentration around countersunk hole in isotropic plates for the various cases of uniformly distributed load, uniformly varying load and harmonic load. In the present study, an attempt is made to investigate the effect of various parameters i.e. countersunk angle, countersunk depth to thickness ratio, thickness to radius ratio and width to radius ratio on the stress concentration with the help of finite element analysis software, ANSYS.

Extensive studies have been performed by Pilkey and Pilkey [1] on the stress concentration of two dimensional plates with holes and notches under different loading conditions. Shivakaumar and Newman [2] conducted three dimensional finite element analyses for plates with straight shank and countersunk holes subjected to various loading conditions. They found that the stress concentration factor for a plate with countersunk hole and subjected to tension is 30 percent higher than that for a straight shank hole while the countersinking has no influence on the bending stress concentration factor. On the basis of the finite element results, stress concentration equations were formulated. Wu and Mu [3] analyzed the stress concentration factor around holes in isotropic and orthotropic plates subjected to uniaxial and biaxial loading. They studied the influence of structural dimension on the SCF and suggested an empirical method for the calculation of SCF which agreed well with the finite element results. Kotousov and Wang [4] derived analytical solutions for 3-d stress distribution around typical stress concentrators in an isotropic plate of arbitrary thickness. They obtained an approximate solution for the through-the-thickness constraint factor in a plate with V-shaped notch having a circular tip. Kotousov et al. [5] reviewed some previous work and attempted to summarize the effect of thickness on the state of stress in plate components. Li et al. [6] performed a detailed 3-d FE analysis in plates and investigated the elastic notch-root fields in plates with different thicknesses and notch configurations subjected to uniaxial tension. Based on extensive FE calculations, Berto et al. [7] presented an analytical solution for the stress field at a notch root in a plate of arbitrary thickness and confirmed that the thickness has a very little effect on the in-plane SCF. She and Guo [8] analyzed the through-the-thickness variation of the SCF along the wall of elliptical holes in isotropic plates subjected to a remote tensile stress with the help of finite element method and some useful characteristics were revealed. Wharley [9] determined the elastic stress concentration factors for countersunk holes by determining the local stresses in plane hole specimens using birefringent-plastic coating method. Shivakumar et al. [10] and Bhargava and Shivakumar [11] conducted a detailed a 3-d FE analysis on countersunk holes in plates subjected to tension for a wide range of countersunk depths, countersunk angles, plate thicknesses, and plate widths. On the basis of FE results, a general equation for determination of stress concentration was proposed and verified. Again, Bhargava and Shivakumar [12] extended their previous research to develop a general equation for the strain concentration factor. Jain and Mittal [13] used FE method to analyze the effect of D/A ratio on the distribution of stresses and deflection in isotropic, orthotropic and laminated composite plates containing a circular hole at the center and subjected to transverse static loading. Darwish et al. [14] introduced a corrected equation for the stress concentration factor of a uniaxially loaded isotropic plate with a countersunk hole at the center. Darwish et al. [15] further extended his research to investigate the in-plane stress concentration factor in countersunk rivet hole in orthotropic, laminated plate under uniaxial tension load. In this paper, the effect of countersunk depth, plate thickness, countersunk angle

P. K. Saini is an Associate Professor of Mechanical Engineering at National Institute of Technology, Kurukshetra, 132119 India (phone: 0091-1744-228880; fax: 0091-1744-238050; e-mail: pksaini@ nitkkr.ac.in).

T. Agarwal is with the Mecanical Engineering Department, National Institute of Technology, Kurukshetra, 132119 India (phone: 0091-1744-233469; fax: 0091-1744-238050; e-mail: tarun4ever@gmail.com).

and plate width on the stress concentration around countersunk hole in plates subjected to various kinds of loading has been explored.

II. Problem Description

The configuration of the plate with a countersunk hole and its main geometric features are shown in Fig. 1. The figure shows the reference coordinate system x-y-z, and defines the plate width (2w), length (2h) and thickness (t). The thickness of the countersunk hole is divided into two portions: the countersinking thickness (C_s) and the straight shank thickness (b). The plate thickness is defined as $t=C_s+b$. The straight shank radius is (r) and the countersink angle is (θ_c).

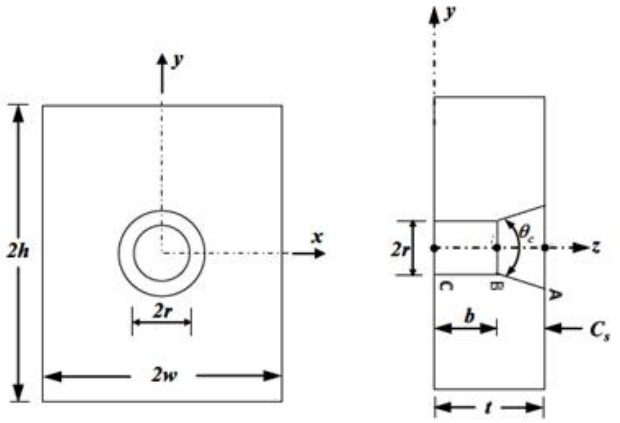

Fig. 1 Configuration of a countersunk hole

In most industrial applications the countersink angle is in the range of 80°-120°. Steel with modulus of elasticity E =210 GPa and Poisson's ratio ν=0.3 is considered for the modeling of the plate of the present study. The boundary conditions of the quarter model were imposed by constraining the displacement in the x-direction (u_x) at x=±w and the displacement in the y-direction (u_y) at y=±h. These constraints account for the planes of symmetry of the full model. To prevent the motion in the z-direction, the out of plane displacement (u_z) was constrained at all the four edges. The plate is subjected to the following types of loadings, i.e.

- Uniformly distributed load
- Uniformly varying load
- Functionally varying load

The schematic representation of all the three loadings has been shown in Fig. 2. In the presence of singularity, the maximum stress occurs at a point along the circumference of hole. Since stress in y-direction is greater than the stress in x-direction, the stress concentration factor is based on σ_y. The stress concentration $K_t(z)$ is stated as

$$K_t(z) = \frac{\text{Stress at a point in the presence of singularity}}{\text{Maximum stress when singularity is not present}}$$

The stress concentration factor is defined as the maximum of $K_t(z)$.

III. Analysis

A. Model Preparation

A linear finite element stress analysis is conducted with the help of code written in ANSYS Parametric Design Language (APDL). A 3-D hexahedron element, specified as SOLID45 has been chosen to generate mesh in the volumes. In order to achieve accurate results for the stress concentration factor in the neighborhood of the hole, more elements are used near the region close to hole boundary compared to the region far away from the hole i.e. a finer mesh near the hole and a coarser mesh elsewhere is used. A quarter symmetric meshed finite element model has been shown in Fig. 3.

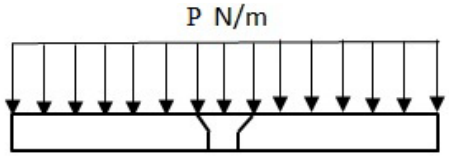

Fig. 2 (a) Schematic representation of a uniformly distributed load

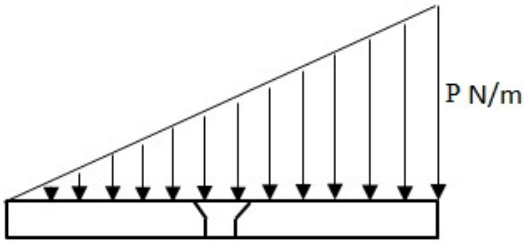

Fig. 2 (b) Schematic representation of a uniformly varying load

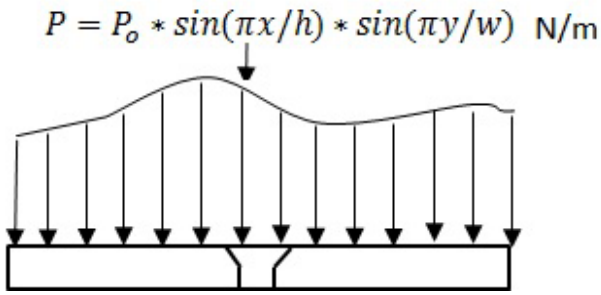

Fig. 2 (c) Schematic representation of a functionally distributed load

B. Mesh Refinement

Mesh refinement study is conducted to optimize the mesh size. Four different models - Baseline, fine, finer and finest mesh are considered, each by doubling the number of elements. For each mesh the maximum stress concentration factor is calculated and is compared with the next finer mesh. It is seen that the baseline mesh and the finest mesh results differ by -0.15 percent. Since the difference is small, the baseline mesh has been used for further studies. Fig. 4 shows the results of the mesh convergence study. It is clearly evident from the Fig. 4 that the mesh size is optimal.

C. Model Validation

Since the entire research is based on the accuracy of FE modeling and its results, the verification of FE code is very

essential. The verification analysis has been performed by independently generating FE models and reproducing the results for certain cases in the literature. Results obtained from the finite element simulation run are compared with those obtained from the analytical equations given by Roark [16] which were derived for a plate with a straight shank hole at the center and subjected to end moment. It is clear from the Fig. 5 that the FE results are in agreement the analytical solution with the maximum error of 8.6 percent occurring at r/w=0.06 where r is the hole radius and w is the half-width of plate.

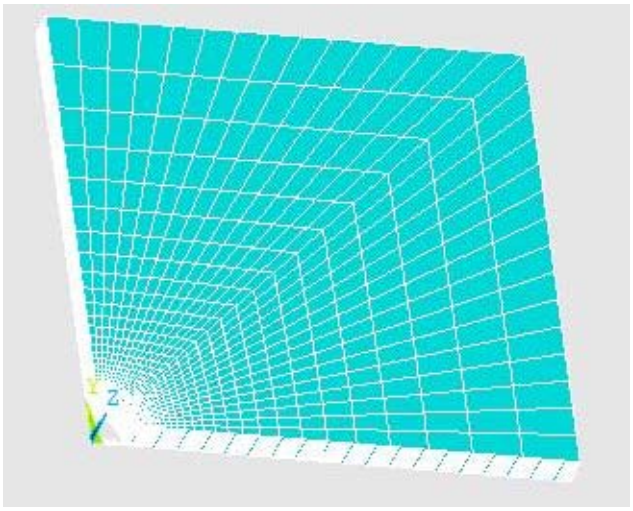

Fig. 3 Quarter symmetric FE model

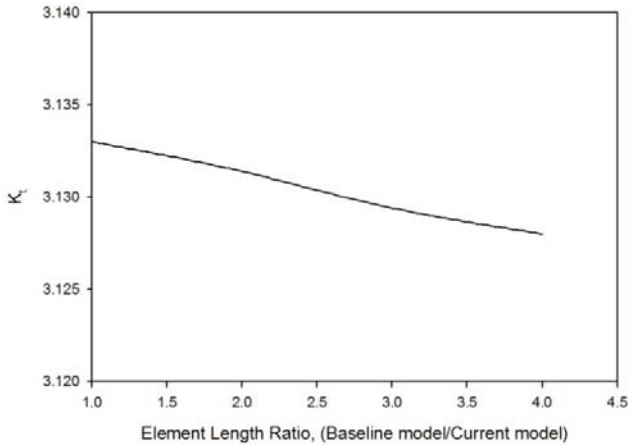

Fig. 4 Plot of K_t for different mesh refinements

Jain and Mittal [13] studied the distribution of stresses and deflection in rectangular isotropic plates with central circular hole under transverse static loading. Fig. 6 compares the finite element results with those obtained by Jain and Mittal [13]. It can be seen that the results obtained from the present model are in good agreement with those of Jain and Mittal [13].

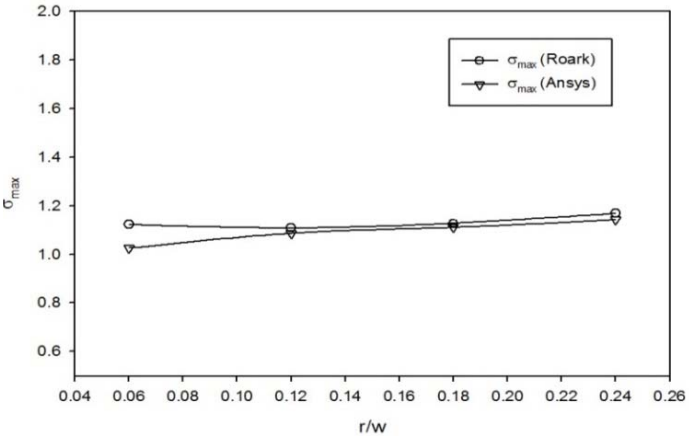

Fig. 5 Verification of FE results with analytical solution

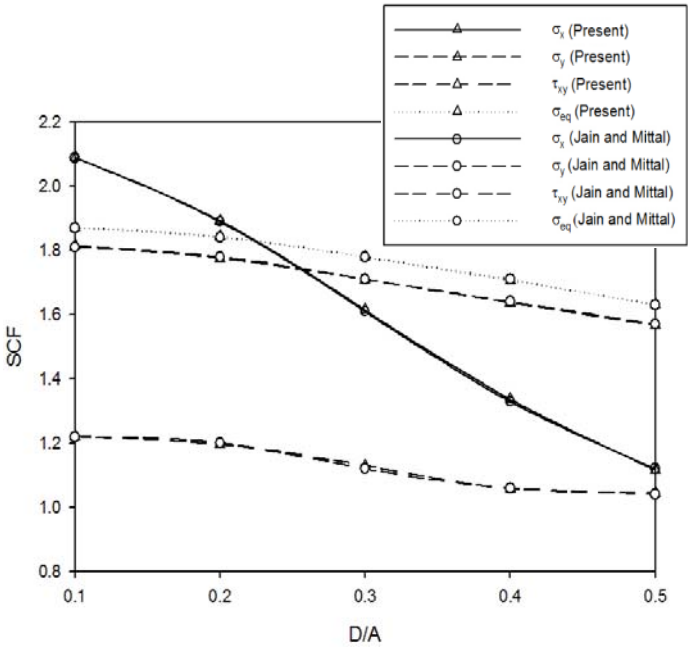

Fig. 6 Verification of FE results with Jain and Mittal [13]

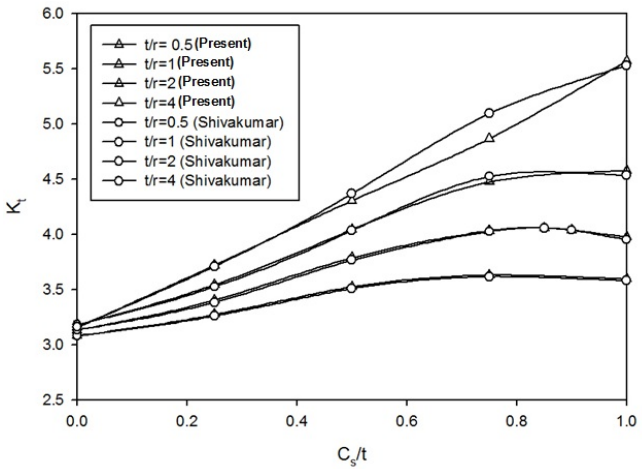

Fig. 7 Verification of FE results with Shivakumar et al. [11]

Shivakumar et al. [11] analysed the stress concentration around countersunk hole in plates subjected to uniaxial tensile loading and its variation with respect to various parameters viz. countersunk depth, countersunk angle, plate thickness and plate width. It is clear from Fig. 7 that the present FE results are in agreement with those of Shivakumar et al. [11] with maximum error of 4.47 percent occurring at Cs/t=0.75 for t/r=4.

IV. Results and Discussion

The results of the comprehensive three dimensional finite analysis that has carried out to determine the stress distribution around countersunk hole in plates for various kind of loadings is presented in this section. The various loadings considered are: (a) Uniformly distributed load (b) Uniformly varying load and (c) Functionally distributed load i.e.

$$P = P_o * \sin(\pi x/h) * \sin(\pi y/w)$$

The finite element analysis has been conducted for a wide range of (C_s/t), t/r, θ_c and w/r parameters to evaluate their effect on stress concentration factor.

A. Effect of Countersunk Depth to Thickness Ratio (Cs/t)

The distribution of Kt(z) along z/t for various countersink depths i.e. 0, 0.25, 0.5, 0.75, 0.9 and 1 is shown in Fig. 8 for h/r=w/r=15, t/r = 1 and θc=100°. Kt(z) is maximum at C and it decreases towards the top continuously irrespective of loading. Kt is maximum for knife edge hole and least for straight shank hole.

For uniformly distributed load, Kt(z) at point C is 1.238~1.525 times Kt(z) at the surface i.e. point A, while for the case of uniformly varying load and functionally distributed load it is in the range of 1.237~1.528 and 1.240~1.537 respectively. The ratio of Kt(z) at point C and Kt(z) at countersunk edge i.e. point B is in the range of 1.297~10.085 for the case of uniformly distributed load while for the uniformly varying load and functionally distributed load, it is in the range of 1.321~9.439 and 1.299~10.082 respectively. Except for the straight shank hole for which the variation of Kt(z) with z/t is linear, the variation is non-linear for countersunk and knife-edge holes.

A. Effect of Countersunk Angle (θc)

Fig. 9 shows the variation of $K_t(z)$ along z/t for countersunk angles ranging from 60° to 120° for h/r=w/r=15, t/r=1 and C_s/t=0.25. A countersunk angle of 100° is used in typical aircraft structures. $K_t(z)$ is maximum at C and it decreases towards the top monotonously. For uniformly distributed load, $K_t(z)$ at point C is 1.208~1.329 times $K_t(z)$ at the surface i.e. point A, while for the case of uniformly varying load and functionally distributed load it is in the range of 1.119~1.327 and 1.121~1.331 respectively.

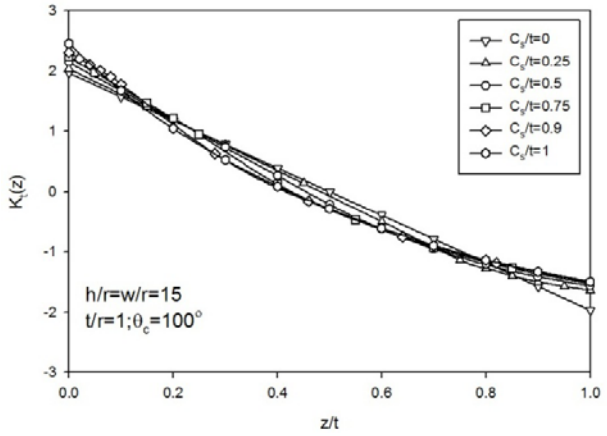

Fig. 8 (a) Effect of Cs/t on SCD for wide plates subjected to UDL

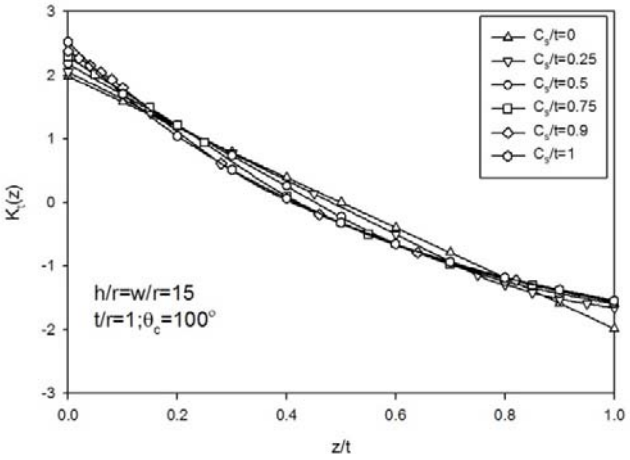

Fig. 8 (b) Effect of Cs/t on SCD for wide plates subjected to UVL

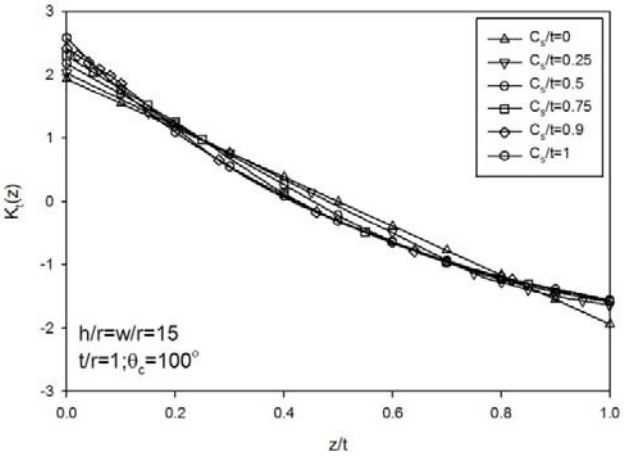

Fig. 8 (c) Effect of Cs/t on SCD for wide plates subjected to FDL

The ratio of $K_t(z)$ at point C and $K_t(z)$ at countersunk edge i.e. point B is in the range of 1.738~1.874 for the case of uniformly distributed load while for the uniformly varying load and functionally distributed load, it is in the range of 1.735~1.88 and 1.739~1.875 respectively. For the straight shank portion, the rate of change of $K_t(z)$ with z/t is higher for higher values of countersunk angle. As soon as the

countersunk portion is reached, the trend changes and the rate of change of $K_t(z)$ with z/t becomes less for higher values of countersunk angle.

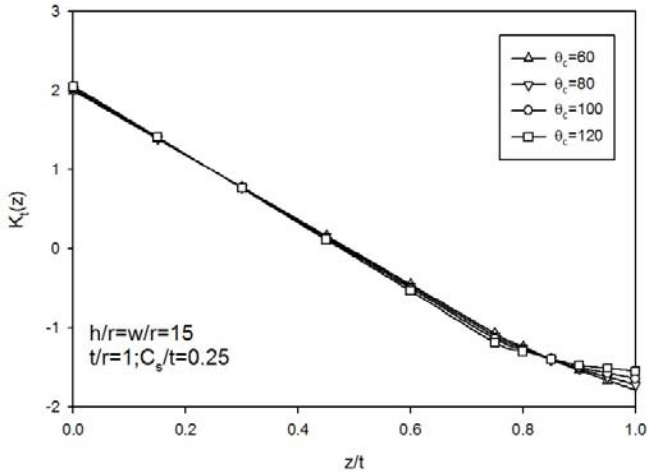

Fig. 9 (a) Effect of θ_c on SCD for wide plates subjected to UDL

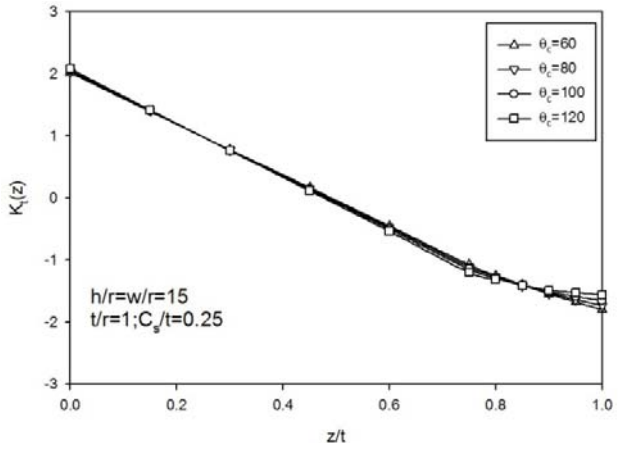

Fig. 9 (b) Effect of θ_c on SCD for wide plates subjected to UVL

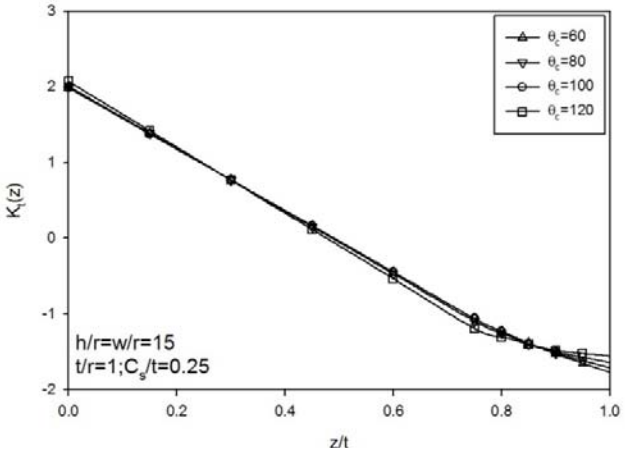

Fig. 9 (c) Effect of θ_c on SCD for wide plates subjected to FDL

B. Effect of Thickness to Radius Ratio (t/r)

Fig. 10 illustrates the effect of t/r on $K_t(z)$ for C_s/t= 0.5. Values of t/r = 0.5, 1 and 2 represent the practical range of hole configurations used in the aircraft industry and $t/r \geq 2$ is used for thick structures such as those found in marine applications. $K_t(z)$ is maximum at C and it keeps on decreasing towards A. For the functionally distributed load, K_t is maximum for t/r=4 while for the uniformly distributed load as well as uniformly varying load, K_t for t/r=2 is slightly higher than that for t/r=4. For uniformly distributed load, $K_t(z)$ at point C is 1.207~1.818 times $K_t(z)$ at the surface i.e. point A, while for the case of uniformly varying load and functionally distributed load it is in the range of 1.21~1.79 and 1.209~1.877 respectively.

The ratio of $K_t(z)$ at point C and $K_t(z)$ at countersunk edge i.e. point B is in the range of 4.538~17.386 for the case of uniformly distributed load while for the uniformly varying load and functionally distributed load, it is in the range of 4.185~16.281 and 4.531~17.362 respectively. Starting from C upto the countersunk edge, the rate of variation of $K_t(z)$ is high and becomes less afterwards. After this distance, the rate of variation of $K_t(z)$ with z/t is observed to become less for higher values for t/r.

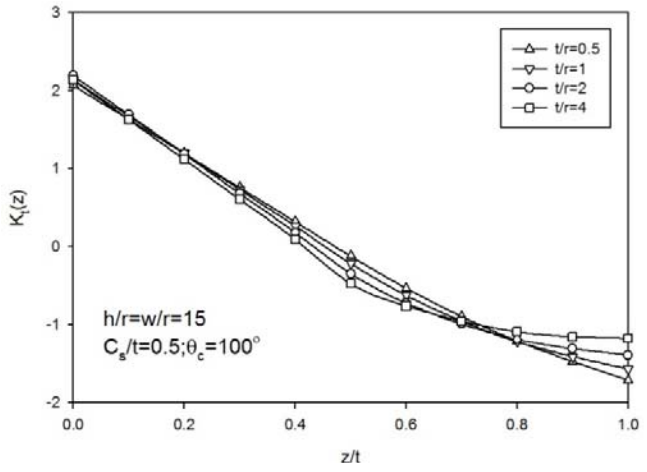

Fig. 10 (a) Effect of t/r on SCD for wide plates subjected to UDL

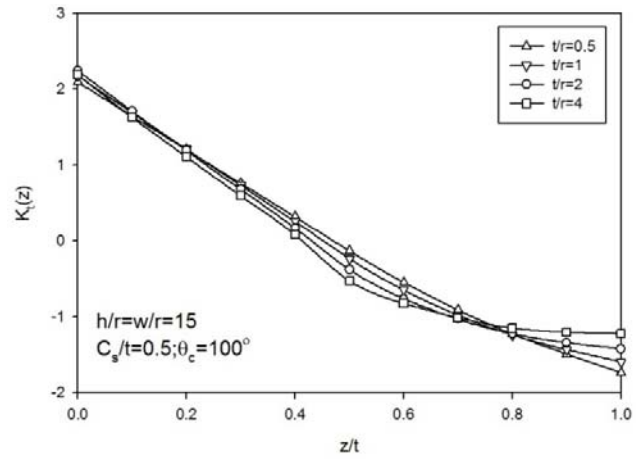

Fig. 10 (b) Effect of t/r on SCD for wide plates subjected to UVL

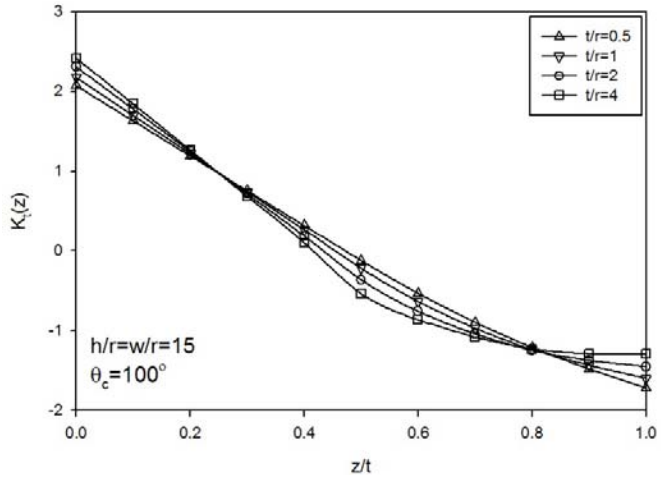

Fig. 10 (c) Effect of t/r on SCD for wide plates subjected to FDL

C. Effect of Width to Radius Ratio (w/r)

Fig. 11 shows the distribution of $K_t(z)$ along z/t for various plate width to radius ratio i.e. 2,3,6,9,12 and 15 for h/r=15, t/r=1 and C_s/t=0.5. The maximum value of $K_t(z)$ occur at point C. K_t is maximum for w/r=15 and least for w/r=2. $K_t(z)$ decreases towards the top continuously. Upto the mid-thickness, the rate of decrease of $K_t(z)$ with z/t is sharp and linear. Beyond that, the variation of $K_t(z)$ with z/t becomes less and non-linear. The value of $K_t(z)$ at point A follows an opposite trend to that at point C i.e. plates for which $K_t(z)$ is minimum at point C are having the maximum value of $K_t(z)$ at point A. For uniformly distributed load, $K_t(z)$ at point C is 1.114~1.365 times $K_t(z)$ at the surface i.e. point A, while for the case of uniformly varying load and functionally distributed load it is in the range of 1.101~1.369 and 1.108~1.37 respectively. The ratio of $K_t(z)$ at point C and $K_t(z)$ at countersunk edge i.e. point B is in the range of 6.442~12.721 for the case of uniformly distributed load while for the uniformly varying load and functionally distributed load, it is in the range of 6.22~11.439 and 6.692~13.445 respectively.

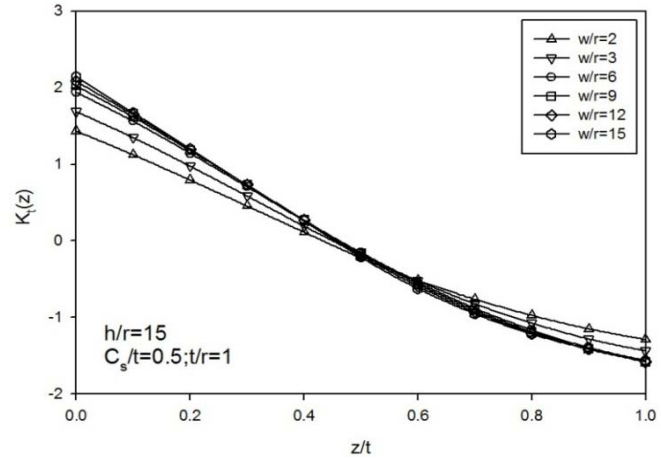

Fig. 11 (a) Effect of w/r on SCD for plates subjected to UDL

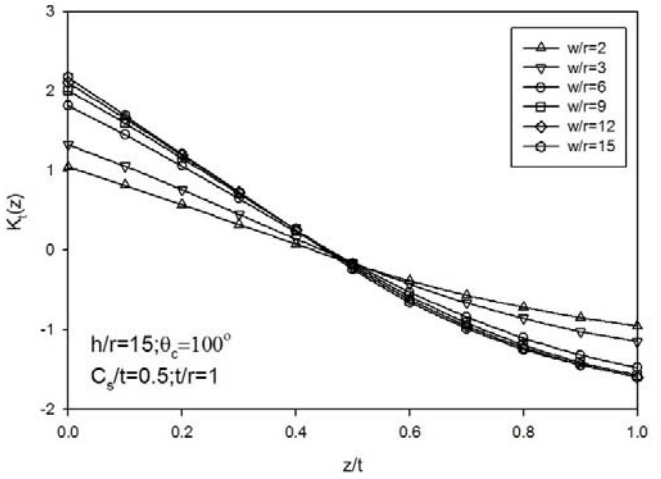

Fig. 11 (b) Effect of w/r on SCD for plates subjected to UVL

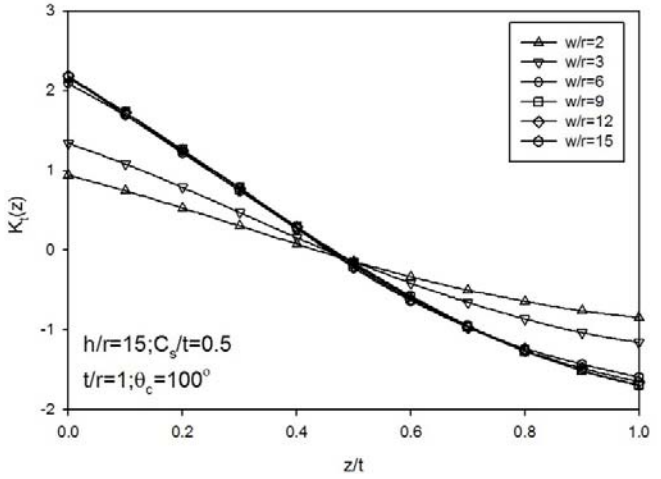

Fig. 11 (c) Effect of w/r on SCD for plates subjected to FDL

V. Conclusion

A comprehensive three dimensional finite element analysis has been performed to study the distribution of stress concentration around straight shank hole and countersunk hole in plates subjected to different kind of loadings i.e. uniformly distributed load, uniformly varying load and functionally distributed load. A finite element analysis code, written in APDL is used for the geometric modeling, finite element modeling and analysis of the problem. An 8-noded hexahedron element, defined as SOLID45 is used for the purpose of simulation. The analysis has been done for a wide range of countersunk depth, plate thickness, countersunk angle and plate width and the behavior of stress concentration is studied with respect to these parameters. Based on the finite element results, it is observed that the maximum value of stress concentration occurs at a particular point i.e. point C and it decreases as we move towards the top along the boundary of countersunk hole. It is found independent of plate width, plate thickness, countersunk depth and countersunk angle. It is also noticed that variation in the stress concentration distribution follows a similar trend for all the three types of loadings. Although the stress values are

different but the change in $K_t(z)$ occurs in the same fashion along the countersunk hole from point A to point C.

NOMENCLATURE

w = half width of the plate
h = half length of the plate
t = thickness of the plate
C_s = thickness of the countersunk portion
b = thickness of the straight shank portion
r = radius of straight shank portion
θ_c = countersunk angle
E = modulus of elasticity
v = Poisson's ratio
u_x = displacement along x direction
u_z = displacement along z direction
$K_t(z)$ = stress concentration at a distance z from the origin
K_t = stress concentration factor
UDL = uniformly distributed load
UVL = uniformly varying load
FDL = functionally distributed load
SCD = stress concentration distribution

REFERENCES

[1] W.D. Pilkey, "Peterson's Stress Concentration Factor," 2nd ed. New York: John Wiley & Sons Inc., 1997.
[2] K.N. Shivakumar, and J.C. Newman, "Stress Concentrations for Straight-shank and Countersunk Holes in Plates Subjected to Tension, Bending, and Pin Loading," *NASA Technical Paper*, pp. 3192, 1992.
[3] H. Wu, and B. Mu, "On stress concentrations for isotropic/orthotropic plates and cylinders with a circular hole," *Composites: Part B,* vol. 34, pp. 127-134, 2003.
[4] A. Kotousov, and C.H. Wang, "Three-dimensional stress constraint in an elastic plate with a notch," *International Journal of Solids and Structures,* vol. 77, pp. 1665-1681, 2002.
[5] A. Kotousov, P. Lazzarin, and F. Berto, "Effect of the thickness on elastic deformation and quasi-brittle fracture of plate components," *Engineering Fracture Mechanics*, vol. 39, pp. 4311-4326, 2010.
[6] Z. Li, W. Guo, and Z. Kuang, "Three-dimensional elastic stress fields near notches in finite thickness plates," *International Journal of Solids and Structures,* vol. 37, pp. 7617-7631, 2000.
[7] F. Berto, P. Lazzarin, and C.H. Wang, "Three-dimensional linear elastic distributions of stress and strain energy density ahead of V-shaped notches in plates of arbitrary thickness," *International Journal of Fracture*, vol. 127, pp. 265–282, 2004.
[8] C. She, and W. Guo, "Three-dimensional stress concentrations at elliptic holes in elastic isotropic plates subjected to tensile stress," *International Journal of Fatigue*, vol. 29, pp. 330-335, 2007.
[9] R.E. Wharely, "Stress-concentration factors for countersunk holes," *Experimental Mechanics,* vol. 5, pp. 257-261, 1965.
[10] K. N. Shivakumar, A. Bhargava, and S. Hamoush, "A general equation for stress concentration in countersunk holes," *CMC,* vol. 6, pp. 71-92, 2007.
[11] A. Bhargava, and K. N. Shivakumar, "Three Dimensional Tensile Stress Concentration in Countersunk Rivet Holes," *The Aeronautical Journal,* vol. 111, pp. 777-786, 2006.
[12] A. Bhargava, and K. N. Shivakumar, "A three-dimensional strain concentration equation for countersunk holes," *Journal of Strain Analysis and for Engineering Design*, vol. 43, pp. 75-85, 2007.
[13] N. K. Jain, and N. D. Mittal, "Finite element analysis for stress concentration and deflection in isotropic, orthotropic and laminated composite plates with central circular hole under transverse static loading," *Materials Science and Engineering, A*, vol. 498, pp. 115-124,2008.
[14] F. Darwish, M. Gharaibeh, and G. Tashtoush, "A modified equation for the stress concentration factor in countersunk holes," *European Journal of Mechanics- A/Solids*, vol. 36, pp. 94-103, 2012.
[15] F. Darwish, M. Gharaibeh, and G. Tashtoush, "Stress concentration analysis for countersunk rivet holes in orthotropic plates," *European Journal of Mechanics- A/Solids,* vol. 37, pp. 69-78, 2013.
[16] W. C. Young, and R. G. Budynas, "Roark's Formulas for Stress and Strain," 7th Edition. New York: McGraw-Hill, p.786, 2002.